

Critical and slow dynamics in a bulk metallic glass exhibiting strong random magnetic anisotropy

Q. Luo, D. Q. Zhao, M. X. Pan, and W. H. Wang^{a)}

Institute of Physics, Chinese Academy of Sciences, Beijing 100080, People's Republic of China

(Received 25 October 2007; accepted 2 December 2007; published online 9 January 2008)

The nature of the magnetic state of strong random magnetic anisotropy (RMA) remains elusive. It is unclear whether the RMA and the Ising spin glass systems belong to the same class or not. Here, we demonstrate, by investigations of the static, critical, and slow dynamic properties of a Dy-based bulk metallic glass (BMG), the RMA can be classified to a universal class of glass different from Ising spin glass. The results have implication for understanding the connection between RMA and spin glass and the subtle role of anisotropy in the magnetic transition of disorder and frustrated systems. On the other hand, our study has the significance in developing efficient BMGs for functional applications. © 2008 American Institute of Physics. [DOI: 10.1063/1.2827198]

The collective and slow dynamics of the spin glass¹ (SG) and random magnetic anisotropy²⁻⁴ (RMA) have been extensively studied. One of the controversial issues for both systems is whether they belong to the same class. In SG, random competing exchange interaction (J) plays the dominant role, and only slight anisotropy D ($\ll J$) exists which plays a subtle role in the nature of transition such as the critical exponents and slow dynamics.^{1,6,7} However, the situation becomes more complicated in RMA of which the ground state is determined by the competition between D and J . A correlated speromagnet (CSM) for $D/J \ll 1$ and speromagnetic (SM) state for $D/J \gg 1$ were suggested.³ At an intermediate anisotropy to exchange ratio, Billoni *et al.*⁹ suggests a Heisenberg-type spin glass (HSG) behavior. Theoretical works^{10,11} shown that, in the limit of $D \rightarrow \infty$, the RMA possesses the Ising spin glass (ISG) behavior. However, the evidence of directly relating energy structure and critical dynamics of the strong RMA to an ISG is elusive.³⁻⁸ The heavy rare earth based bulk metallic glasses^{12,13} (BMGs) not only possess high thermally stability, the facility of bulk form, and excellent mechanical property, but also have profuse magnetic structure for promising functional applications. Although good candidates as magnetic refrigerants have been suggested,¹³ the magnetic transition and slow dynamics behavior of these BMGs have not been studied yet. The understanding of these issues has importance in fundamental physics of glasses and in developing materials for functional usage.

In this paper, we study the transition and slow dynamics of a Dy-based BMG taken as an ideal strong RMA. We compare our results with the theoretical works about RMA and ISG to settle the question of the connection between RMA and ISG. From the magnetic measurements, a transition line in the H - T plane in the form of Almeida-Thouless (A-T) line¹⁴ has been obtained in the low field suggesting the Ising property, and a crossover behavior is observed in higher field region that may associate with HSG-like behavior. The relaxation of low field ac susceptibility above T_g reflecting the dynamic spin correlation is analyzed using an equation similar to the Ogielski function.¹⁵

The typical Dy-based BMG $\text{Dy}_{40}\text{Al}_{24}\text{Co}_{20}\text{Y}_{11}\text{Zr}_5$ was prepared in a form of a rod of 3 mm in diameter by arc melting pure constituent elements in a Ti-gettered argon atmosphere. Their amorphous nature was ascertained by x-ray diffraction, transmission electron microscope, and differential scanning calorimeter.¹³ The temperature (T) and field dependence of magnetization were measured in Physical Properties Measurement System, PPMS 6000.

Figure 1(a) shows T dependence of the magnetization under a large field range of 100 Oe–2 T. The zero field cooled (ZFC) branch was measured on heating after initially cooling from 200 to 2 K in zero field. The field cooled (FC) branch was measured on heating after initially cooling to 2 K in the same measuring field. Each ZFC curve exhibits a cusp, and near about the same temperature, bifurcation appears between the FC and ZFC branches. The peak temperature of ZFC curve is regarded as the spin freezing temperature T_f . For ISG, an A-T line¹⁴ was theoretically suggested as a field-dependent transition line and observed for many conventional SGs. From plotting T_f vs $H^{2/3}$ [Fig. 1(b)], it is clearly seen that the A-T line is satisfied well in the low field region. However, a crossover behavior occurs in above 4000 Oe. To further conform this crossover, we also analyze the field

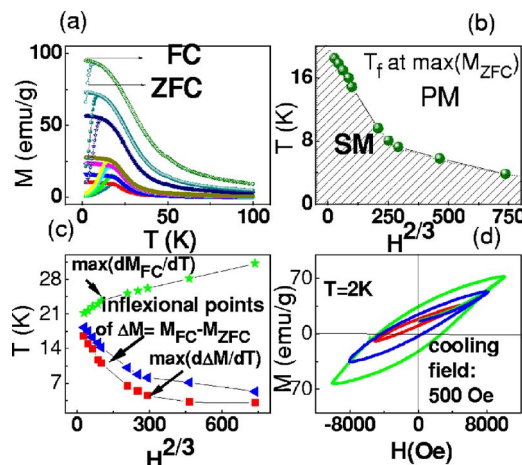


FIG. 1. (Color online) (a) T dependence of the ZFC and FC magnetizations (b) Field dependence of T_f . (c) Field dependence of other characteristic temperatures. (d) Magnetic hysteresis loop at 2 K after field of 500 Oe cooling between ± 5080 , ± 8080 , and ± 10080 Oe.

^{a)} Author to whom correspondence should be addressed. Electronic mail: whw@aphy.iphy.ac.cn.

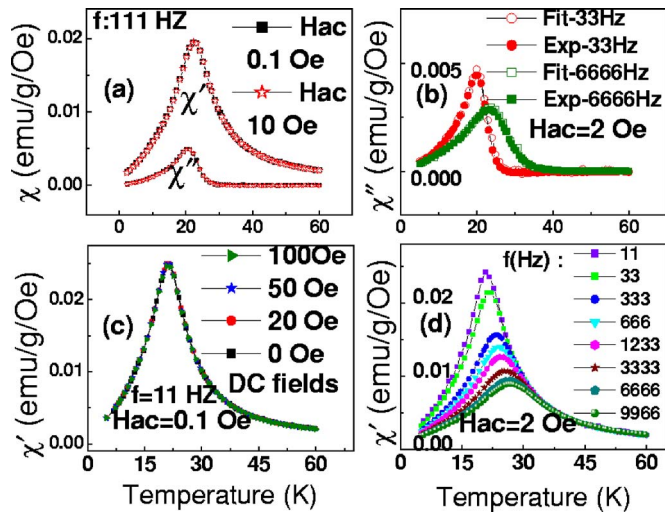


FIG. 2. (Color online) (a) The χ' at 111 Hz with different ac fields (b) χ' gotten from experiment directly compared with obtained from Lendgren relation under an ac magnetic field of 2 Oe. (c) The χ' under different dc fields. (d) The χ' at frequencies ranging from 10 to 10^4 Hz.

dependence of other characteristic temperatures as listed in Fig. 1(c). The results indicate that the longitudinal magnetization of the RMA in the low field region shows an ISG-like behavior, while in high field, it may transform into a HSG-like state. Previous work⁴ of a strong RMA showing only the A-T line without crossover might be due to the limited field range used (<300 Oe).

Similar anisotropy-induced crossover has been suggested¹⁶ in a mean-field model for a HSG with weak random Dzyaloshinsky-Moriya anisotropy. In terms of the above results, it is possible to conclude that some common characteristics exist among real HSG, ISG, and strong RMA in the low field limit. Figure 1(d) displays the hysteresis loops after cooling the glass to 2 K in 500 Oe. All the curves shift perpendicularly above the origin and the centers move down with increasing range of fields suggesting the strong RMA, which is different from some archetypal SGs where displaced loops along the field axis are observed.¹

Figure 2(a) shows the ac susceptibility at 111 Hz with different probing ac fields of 0.1 and 10 Oe. The susceptibility of 10 Oe superposes on the curve of 0.1 Oe in the whole T range suggesting the linear response to the field perturbation. This is different from that of some weak RMA (Ref. 17) which shows strong dependence of the ac susceptibility on the probing fields. Figure 2(c) displays the χ' at 11 Hz with ac field of 0.1 Oe under different dc fields of 0, 20, 50, and 100 Oe. The curves are nearly the same in this low dc field region. The ac susceptibility of strong RMA is stronger to external fields than that of the weak RMA (Refs. 8 and 17), in which usually several gauss of dc fields can make obvious difference on shape of the curve.

The T dependent χ' at different frequencies from 10 to 10^4 Hz under 2 Oe are displayed in Fig. 2(d). The frequency sensibility of $T_f(\omega)$, represented by $\Delta T_f(\omega)/[T_f(\omega)\Delta \log 10\omega]$, is determined to be ~ 0.036 , which is close to that of a conventional SG. Well above T_f , in the paramagnetic regime, the frequency dependent susceptibility follows the Debye relation well. Near T_f , for random and strong frustration system, a broad distribution of relaxation time is expected. A simple relationship between χ' and χ'' is obtained,¹⁸ $\chi''(\omega) = (\pi/2)d\chi'(\omega)/d \ln \omega$. Figure 2(b)

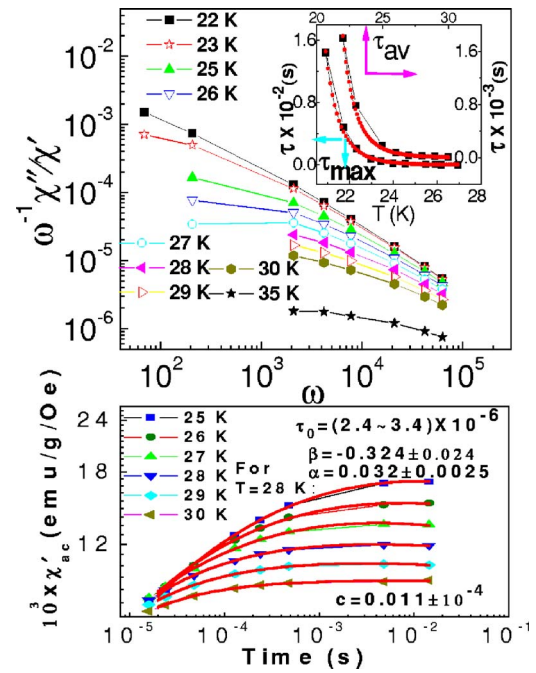


FIG. 3. (Color online) (a) $\omega^{-1}(\chi''/\chi')$ vs ω at different temperatures in a log-log diagram. The inset shows relaxation time τ_f and τ_{av} vs T , and the red lines were obtained by fitting of a power law. (b) Relaxation of $\chi'(t)$ determined above T_g . The continuous red lines are the fitting lines.

shows that this relationship is precisely obeyed for the whole T range measured at both 33 and 6666 Hz indicating the broad relaxation distribution.

The ω dependent maximum in χ' indicates T_f . For critical slowing down dynamics, it is expected that the correlation length diverges at the transition T and the relaxation time obeys the relationship^{1,15}

$$\tau_{\max} = \tau^* (T_f/T_g - 1)^{-z\nu}, \quad (1)$$

where τ_{\max} is the maximum of the relaxation time. For conventional SG, the $z\nu$ is between 4 and 13, and τ^* is $\sim 10^{-10} - 10^{-13}$ s. As shown in Fig. 3(b), the best fit to Eq. (1) gives $\tau^* = 10^{-6}$ s, $T_g = 16.6$ K, and $z\nu = 7.16$. It is noted that the value of τ^* is much larger than that of conventional SG, and $z\nu$ is comparable with the value obtained from Ogielski's simulation for ISG.¹⁵ The much larger value of τ^* gives the fundamental difference between the RMA and SG system.

To further understand the critical dynamics, we analyze the data according to the relation derived by Ogielski, $\lim_{\omega \rightarrow 0} (\omega^{-1}\chi''(\omega)/\chi'(\omega)) = \tau_{av}$, where τ_{av} is the average correlation time. Figure 3(a) shows $\omega^{-1}(\chi''/\chi')$ vs ω in a log-log diagram near and above T_g . At given T , $\omega^{-1}(\chi''/\chi')$ approaches a frequency independent value in the low frequency limit. By fitting the values extracted from the low frequency limit according to Eq. (1), the τ^* , T_g , and $z\nu$ are determined to be 3.64×10^{-6} s, 16.1 K, and 6.2, respectively. The values of τ^* and T_g are nearly the same with those obtained with τ_{\max} but the $z\nu$ gets smaller. It is noted that τ_{av} is about one order smaller than τ_{\max} which further demonstrates that the relaxation distribution is really broad. Simulations usually perform on system close to equilibrium. In the linear response regime, above T_g , the time dependence of the zero field $\chi'(t)$ in equilibrium directly reflects the behavior of the dynamic spin correlation function.^{15,19} For ISG in thermal

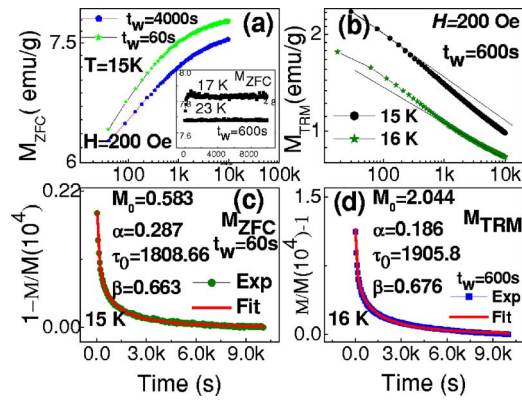


FIG. 4. (Color online) (Color online) (a) Growth of M_{ZFC} in a log-log diagram. (b) Decay of M_{TRM} in a log-log diagram, the black straight lines are guide for the eyes. (c) Evolution of $(M_{ZFC}(10^4) - M_{ZFC}) / M_{ZFC}(10^4)$, the red line is the best fit by $\bar{M} = M_0 t^{-\alpha} e^{-(t/\tau_0)^\beta}$. (d) Evolution of $(M_{TRM}(10^4) - M_{TRM}) / M_{TRM}(10^4)$ and the red fitting line.

equilibrium, it was suggested that the dynamic correlation function follows the empirical formula,

$$q(t) = ct^{-\alpha} e^{-(t/\tau^*)^\beta}, \quad (2)$$

where c , α , τ^* , and β are T dependent parameters. For strong RMA, Chakrabarti¹¹ indicated that in three dimensions ($d=3$) in the limit of infinite anisotropy strength, the RMA exhibits a finite-temperature phase transition to a nonferromagnetic ground state, with critical exponents consistent with those of the $d=3$ short-range ISG. Figure 3(b) shows the zero field time dependent susceptibility in a log-log diagram above T_g ($T/T_g \sim 1.5-1.8$) to reflect the equilibrium dynamics. Figure 3(b) shows the fits of Eq. (2) to the experimental data. The data are fitted very well in the entire time domain. The parameters c , τ^* , α , and β are determined to be $(0.016 \pm 4) \times 10^{-4}$, 0.105 ± 0.003 , $3.8 \times 10^{-(4 \pm 1)}$ s, and -0.18 ± 0.0033 at 26 K. The results show that Eq. (2) describes, not only the time dependence of $q(t)$ from the simulation for ISG, but also the time dependence of $\chi'(t)$, and thus related $q(t)$ for strong RMA.

Below T_g , the relaxation is affected by aging that is revealed by the dependence of the response on the waiting time.^{1,20,21} However, there are yet no theoretical attempts dealing with the aging behavior of the strong RMA systems. To understand the slow dynamics, the time dependence of the M_{ZFC} and thermoremanent magnetization (TRM) of the metallic glass was carried out. The time dependence of M_{ZFC} was performed as follows: the sample was cooled to the measuring temperature T_m in zero field; after waiting for t_w , the field was turned on and the magnetization was recorded as function of time. For the TRM measurement, the sample was first cooled from a temperature from well above T_g to T_m under 200 Oe; after a wait time t_w , the external field was switched off and the magnetization was recorded. Figure 4(a) shows that M_{ZFC} depends on the waiting time and, with increasing waiting time, the magnetization curve falls into a lower level. It is found that a power law times a stretched exponential function fits both the growth of M_{ZFC} and decay of M_{TRM} over the entire time interval very well, \bar{M}

$= M_0 t^{-\alpha} e^{-(t/\tau_0)^\beta}$, where \bar{M} is the normalized magnetization as labeled in Figs. 4(c) and 4(d). This behavior is different from the simulation results of Ogielski and experimental results for an ISG reported, both of which show algebraic dependence.^{15,21} In fact, the curvature of the curves in the log-log diagrams in Fig. 4(a) and 4(b) indicates that the time responses deviate from the logarithmic and algebraic dependence. We also fit results for slow dynamics at several other temperatures with the same form well, and similar form has been used to a metallic spin glass in the immediate vicinity of T_g .¹⁵

Our results provide several clues about the nature of RMA and its relationship with ISG. The RMA indicates critical slowing down to SM structure with a finite $T_g = 16.6$ K. Also, it shares many common features with ISG, such as a maximum in M_{ZFC} , where the M_{ZFC} and M_{FC} are exhibiting bifurcation, nondiverging susceptibility, nonexponential relaxation near T_g , hysteresis, and the A-T line in the low field region. On the other hand, there are major differences between the RMA and ISG. The relaxation time near T_g is much larger than that of conventional SG. The relaxation below T_g does not accord with the theoretical prediction and experimental work of real ISG. We notice that the dominant role of strong RMA in the glassy alloy is different from the random and frustration of exchange coupling in ISG. Further, in the simulation of RMA, the ferromagnetic exchange interaction and the assumption that $D \rightarrow \infty$ are usually adopted, while in practical amorphous magnets, D is finite and the contribution of negative J to critical dynamics may act a role.

Financial support from the NSF of China (Nos. 50621061 and 50671118) and MOST 973 (No. 2007CB613904) is gratefully acknowledged.

¹K. Binder and A. P. Young, Rev. Mod. Phys. **58**, 801 (1986).

²C. Jayaprakash and S. Kirkpatrick, Phys. Rev. B **21**, 4072 (1980).

³E. M. Chudnovsky, W. M. Saslow, and R. A. Serota, Phys. Rev. B **33**, 251 (1986); E. M. Chudnovsky, J. Appl. Phys. **64**, 5770 (1988).

⁴B. Dieny and B. Barbara, Phys. Rev. Lett. **57**, 1169 (1986); D. J. Sellmyer and S. Nafis, *ibid.* **57**, 1173 (1986); R. Fisch, Phys. Rev. B **42**, 540 (1990).

⁵R. I. Bewley and R. Cywinski, Phys. Rev. B **54**, 15251 (1996).

⁶F. Bert, V. Dupuis, and J.-P. Bouchaud, Phys. Rev. Lett. **92**, 167203 (2004).

⁷D. Petit, L. Fruchter, and I. A. Campbell, Phys. Rev. Lett. **88**, 207206 (2002).

⁸T. Saito and T. Tsushima, J. Magn. Magn. Mater. **130**, 347 (1994).

⁹O. V. Billoni and F. A. Tamarit, Phys. Rev. B **72**, 104407 (2005).

¹⁰J. H. Chen and T. C. Lubensky, Phys. Rev. B **16**, 2106 (1977).

¹¹A. Chakrabarti, Phys. Rev. B **36**, 5747 (1987).

¹²W. H. Wang, J. Appl. Phys. **99**, 093506 (2006); W. H. Wang, Prog. Mater. Sci. **52**, 540 (2007).

¹³Q. Luo, D. Q. Zhao, M. X. Pan, and W. H. Wang, Appl. Phys. Lett. **88**, 181909 (2006); **89**, 081914 (2006); **90**, 211903 (2007).

¹⁴J. R. L. de Almeida and D. J. Thouless, J. Phys. A **11**, 983 (1978).

¹⁵A. T. Ogielski, Phys. Rev. B **32**, 7384 (1985); P. Granberg, P. Svedlindh, P. Nordblad, L. Lundgren, and H. S. Chen, Phys. Rev. B **35**, 2075 (1987).

¹⁶G. Kotliar and H. Sompolinsky, Phys. Rev. Lett. **53**, 1751 (1984).

¹⁷T. Saito and K. Hanashima, J. Magn. Magn. Mater. **310**, 1540 (2007).

¹⁸L. Lundgren, P. Svedlindh, and O. Beckman, J. Magn. Magn. Mater. **25**, 33 (1981).

¹⁹A. Keren, Phys. Rev. Lett. **89**, 107201 (2002).

²⁰P. Nordblad, P. Svedlindh, and L. Sandlund, Phys. Rev. B **33**, 645 (1986).

²¹A. Ito and H. Aruga, Phys. Rev. Lett. **57**, 483 (1986).